

AD-A163 546

NUSC Technical Document 7181  
13 June 1984

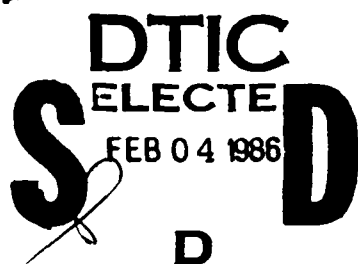
(2)

# High Resolution Bottom Backscatter Measurements

A Paper Presented at the  
107th Meeting of the Acoustical Society of  
America, 8 May 1984, Norfolk, Virginia

W. I. Roderick  
Research & Technology Staff

R. K. Dullea  
Surface Ship Sonar Department



**Naval Underwater Systems Center**  
Newport, Rhode Island / New London, Connecticut

Approved for public release; distribution unlimited.

86 2 3 109

## PREFACE

This work was accomplished under NUSC Project No. A67001, "Weapons Environmental Acoustics Program -- Project WEAP," Principal Investigator, W. I. Roderick (Code 10). The sponsoring activity is the Naval Sea Systems Command, C. D. Smith (SEA-63R), Director. Funding is provided under Program Element 62759N, Subproject Program No. SF59-554, R. L. Martin (NORDA 110A), Manager.

The authors wish to thank J. M. Syck (Code 333) and J. B. Chester (Code 333) for their assistance in the analysis of the bottom contour data and associated roughness spectrum.

REVIEWED AND APPROVED: 13 June 1984

*WA Von Winkle*  
W. A. VON WINKLE  
ASSOCIATE TECHNICAL DIRECTOR OF TECHNOLOGY

The authors of this document are located at the  
New London Laboratory, Naval Underwater Systems Center,  
New London, Connecticut 06320.

REPORT DOCUMENTATION PAGE		READ INSTRUCTIONS BEFORE COMPLETING FORM
1. REPORT NUMBER	2. GOVT ACCESSION NO.	3. RECIPIENT'S CATALOG NUMBER
TD 7181	AD-A163 546	
4. TITLE (and Subtitle)  HIGH RESOLUTION BOTTOM BACKSCATTER MEASUREMENTS	5. TYPE OF REPORT & PERIOD COVERED	
	6. PERFORMING ORG. REPORT NUMBER	
7. AUTHOR(S)  W. I. Roderick and R. K. Dullea	8. CONTRACT OR GRANT NUMBER(S)	
9. PERFORMING ORGANIZATION NAME AND ADDRESS  Naval Underwater Systems Center New London Laboratory New London, CT 06320	10. PROGRAM ELEMENT, PROJECT, TASK AREA & WORK UNIT NUMBERS  A67001 PE 62769N	
11. CONTROLLING OFFICE NAME AND ADDRESS  Naval Sea Systems Command Washington, DC 20362	12. REPORT DATE  13 June 1984	
	13. NUMBER OF PAGES  28	
14. MONITORING AGENCY NAME & ADDRESS (if different from Controlling Office)	15. SECURITY CLASS. (of this report)  UNCLASSIFIED	
	15a. DECLASSIFICATION/DOWNGRADING SCHEDULE	
16. DISTRIBUTION STATEMENT (of this Report)  Approved for public release; distribution unlimited.		
17. DISTRIBUTION STATEMENT (of the abstract entered in Block 20, if different from Report)		
18. SUPPLEMENTARY NOTES		
19. KEY WORDS (Continue on reverse side if necessary and identify by block number)  Acoustic Scattering                                  High Resolution                                  Sand Dollar Azimuth Angle                                        Low Grazing                                      Scattering Strength Bottom Reverberation                                North Atlantic                                    Shallow Water Frequency Dependence                                Project WEAP High Frequency                                        Refractive Caustic		
20. ABSTRACT (Continue on reverse side if necessary and identify by block number)  This document contains the slide presentation entitled "High Resolution Bottom Backscatter Measurements" given at the 107th meeting of the Acoustical Society of America on 8 May 1984 in Norfolk, VA.  Acoustic bottom backscattering measurements and the corresponding geo-acoustic properties of the ocean bottom are presented for an experiment conducted in the shallow water of the North Atlantic. The bottom scattering		

5.03 10/17/78 Jea  
20. Continued:

strength data, which were obtained with a high resolution (narrow beamwidth) parametric sonar, were measured as a function of frequency (5 to 20 kHz), grazing angle ( $4^{\circ}$  to  $11^{\circ}$ ), azimuthal angle ( $\pm 55^{\circ}$ ), and pulse length (0.4 to 10 ms). The supporting environmental measurements included box cores for determining the acoustic properties of the sediment and stereo photography for calculating the two-dimensional roughness spectrum of the sea floor. Analyses indicate that the measured reverberation was significantly influenced by the macrobenthos of the area. In particular, nonhomogeneous concentrations of highly reflective sand dollars resulted in bottom scattering strengths that exhibited both range and pulse width dependencies. No strong frequency or grazing angle dependence was observed. In addition, refractive conditions in the water column were found to markedly alter the time dispersive characteristics of bottom reverberation.

## TABLE OF CONTENTS

	Page
LIST OF ILLUSTRATIONS. . . . .	11
INTRODUCTION . . . . .	1
EXPERIMENTAL PROCEDURES AND MEASUREMENTS. . . . .	5
AZIMUTHAL DEPENDENCE OF BOTTOM REVERBERATION . . . . .	7
TIME DEPENDENCE OF BOTTOM REVERBERATION. . . . .	9
BOTTOM SCATTERING STRENGTH VERSUS GRAZING ANGLE. . . . .	11
FREQUENCY VARIATIONS . . . . .	13
COHERENT AND INCOHERENT BOTTOM REVERBERATION . . . . .	17
BOTTOM CONTOUR AND CORRESPONDING ROUGHNESS SPECTRUM. . . . .	19
SAND DOLLAR DISTRIBUTION . . . . .	23
SUMMARY AND CONCLUSIONS. . . . .	25
LIST OF REFERENCES . . . . .	26

Accession For	
NTIS	CRA&I <input checked="" type="checkbox"/>
LITIC	TAB <input type="checkbox"/>
U.Unannounced	<input type="checkbox"/>
Justification	
By	
Distribution/	
Availability Codes	
Dist	Available and/or Special
A-1	



## LIST OF ILLUSTRATIONS

Figure		Page
1	Location of Experiment . . . . .	2
2	Procedures and Measurements for Bottom Backscattering Experiment. . . . .	4
3	Bottom Reverberation vs. Range for Two Azimuth Angles (Frequency: 20 kHz, Pulse Width: 0.4 ms, Ensemble: 100 Pulses). . . . .	6
4	Bottom Reverberation vs. Range as a Function of Ensemble Interval (Frequency: 20 kHz, Pulse Width: 0.4 ms, Angle: 4°) . . . . .	8
5	Bottom Scattering Strength (20 kHz) vs. Grazing Angle as a Function of Pulse Width and Azimuth. . . . .	10
6	Bottom Reverberation vs. Range at Four Frequencies (Pulse Width: 10 ms, Ensemble: 200 Pulses) . . . . .	12
7	Bottom Scattering Strength vs. Frequency (Grazing Angle: 11°, Pulse Width: 10 ms, Ensemble: 200 Pulses) . . . . .	14
8	Coherent and Incoherent Bottom Reverberation . . . . .	16
9	Sample of Bottom Topography at the Experimental Site . . . . .	18
10	Bottom Roughness Spectrum. . . . .	20
11	Sand Dollar Distribution . . . . .	22
12	Bottom Reverberation Summary Highlights. . . . .	24

## HIGH RESOLUTION BOTTOM BACKSCATTER MEASUREMENTS

## INTRODUCTION

A high frequency acoustic boundary reverberation experiment has been conducted in the shallow waters of the North Atlantic. The experiment was jointly performed among several naval centers and academic institutions including NORDA, FWG (Kiel, Germany), the University of Rhode Island, the City College of New York (CCNY), and NUSC.

In a shallow water environment, propagation under refractive or nonrefractive conditions generally involves reflection and scattering from the ocean boundaries. In most instances, the interaction with the boundaries occurs at low grazing angles and it is precisely at these angles where there is a scarcity of acoustic data for understanding the properties of acoustic reverberation. Low grazing angle scattering of high frequency acoustic signals is also a problem area theoretically because of shadowing, multiple scattering, and roughness dimensions on the order of an acoustic wavelength or greater.

Thus, the objectives of the experiment were to measure the low grazing angle backscatter at several frequencies that ranged from 5 to 80 kHz. In support of the acoustic measurements, it was also important to measure the oceanographic conditions of the ocean medium and the statistics of the boundaries to give theoreticians the environmental information to model the acoustic data. In this document, we will describe the bottom backscattering measurements; a companion paper [1] describes the sea surface reverberation measurements.

TD 7181

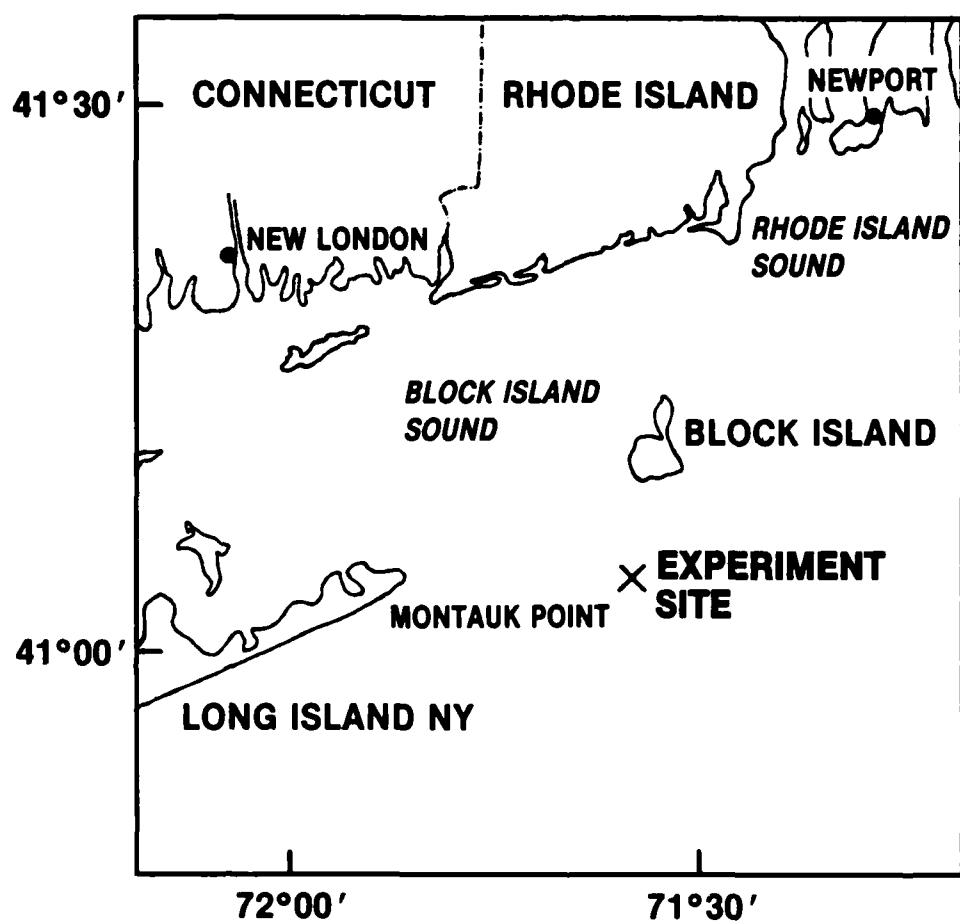


Figure 1. Location of Experiment

The experimental site (figure 1) was located approximately 25 km east of Montauk point, New York, at the southeastern terminus of a drowned barrier spit. The water depth was 35 m and analysis of the sediment types showed both fine and coarse sands were present. The inhomogeneous bottom at the site was further complicated by an abundance of macrobenthic life forms.

TD 7181

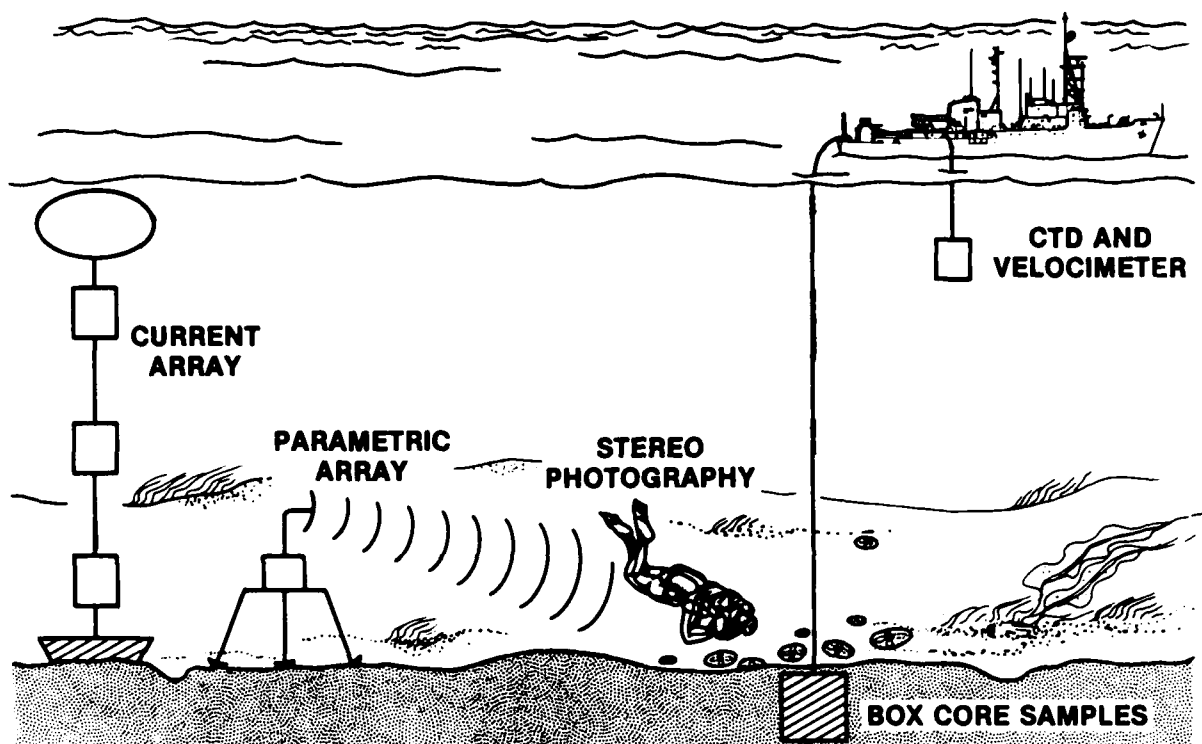


Figure 2. Procedures and Measurements for Bottom Backscattering Experiment

## EXPERIMENTAL PROCEDURES AND MEASUREMENTS

A high resolution parametric array (figure 2) was used as an acoustic projector because its broad bandwidth capabilities, narrow beamwidth, and very low sidelobe levels are important in eliminating multipath propagation effects and obtaining low grazing angle data.

The parametric array had a nominal beamwidth of 3° and was mounted on top of a 7 m high platform. The projector could be rotated in both angles of azimuth and elevation. The signal generation and receiving system were hard-wired to the research ship by a multiconductor coaxial single armored cable. The research ship was positioned in a four-point mooring and hydrophones were suspended from the ship to receive the refracted and bottom-reflected signals. For in-situ ray arrival determination and subsequent propagation loss predictions, conductivity, temperature, and depth (CTD) measurements were performed periodically during the acoustic experimentation. Velocimeter casts supplemented the CTD data. Three vector current meters measured the flow near the ocean bottom, at the source depth, and near the ocean surface. The sediment and faunal samples were obtained from box cores, and the sediment geoacoustic properties were obtained from scuba diver collected sediment cores. Subsequent analysis of these samples was performed by Michael Richardson of NORDA and John Tietjen of CCNY [2]. Divers also collected overlapping stereo pairs to determine the topography of the bottom interface. During a typical measurement sequence, the parametric array would be projected at the ocean bottom and the bottom backscatter would be obtained from an insonified area determined by either the transmitted pulse length or the beamwidth of the projector.

TD 7181

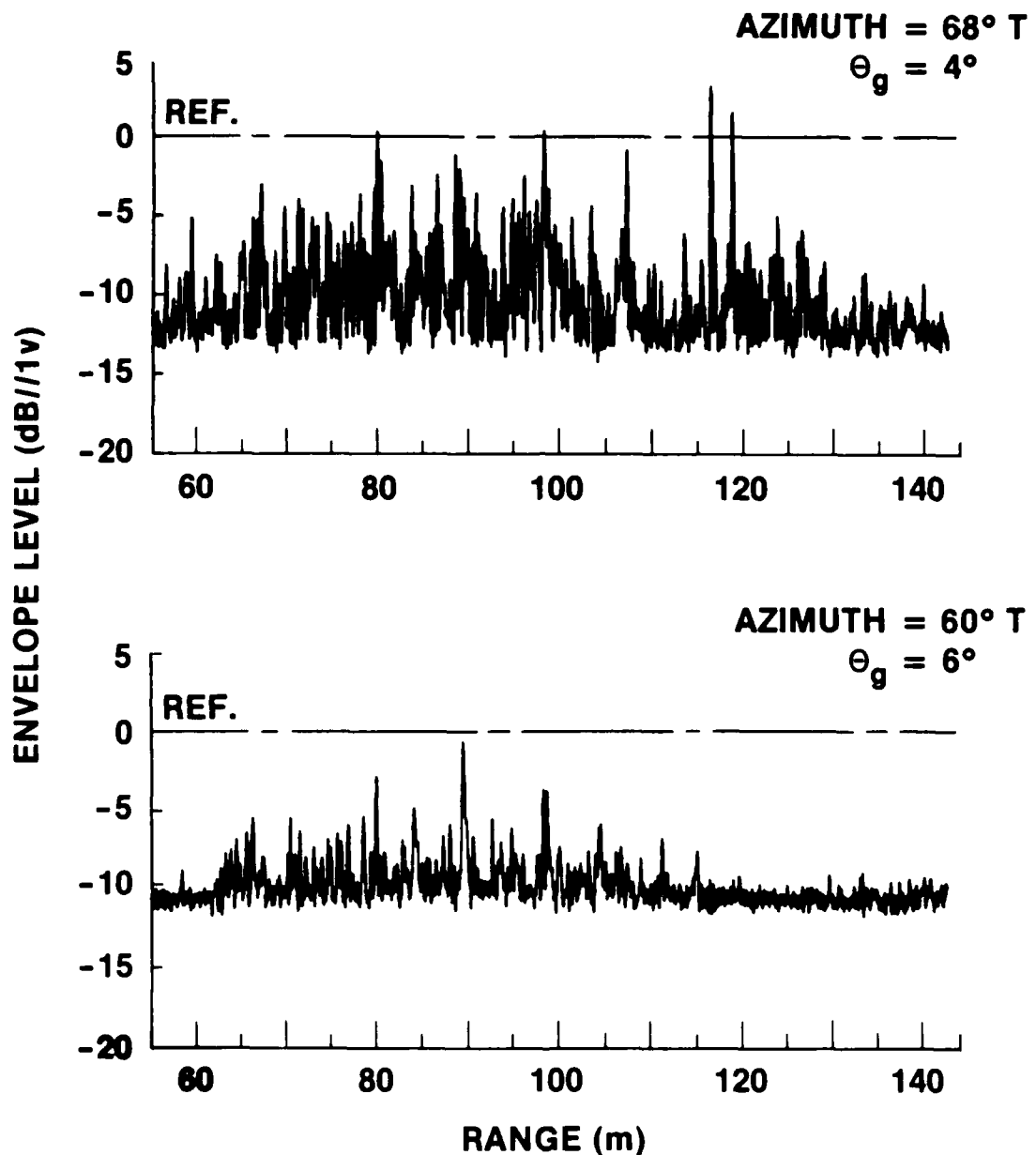


Figure 3. Bottom Reverberation vs. Range for Two Azimuth Angles  
(Frequency: 20 kHz, Pulse Width: 0.4 ms, Ensemble: 100 Pulses)

## AZIMUTHAL DEPENDENCE OF BOTTOM REVERBERATION

A high resolution 0.4 ms pulse was used to probe the bottom at different grazing and azimuth angles. In figure 3, bottom reverberation at 20 kHz is compared for two azimuth angles (relative to the parametric source), which differed by 8°. The discrete scattering "highlights," which were obtained from an ensemble average of 100 pulses, have a range resolution of 0.3 m and a corresponding insonified bottom area of approximately 1 m<sup>2</sup>. The maximum response axis (MRA) of the source was in the vicinity of 110 to 120 m for both azimuth angles. The 2° difference in bottom grazing angles was primarily the result of changes in sound speed refractive conditions between the time measurements were obtained.

The two amplitude scales are equivalent and, in conjunction with the 0 dB reference lines, enable a relative comparison of both the strength and the distribution of individual scattering highlights for the two azimuth angles as a function of range. In general, scattering along the 68° bearing was considerably denser and stronger than at 60°. Relative differences of 5 to 10 dB between the two azimuths are observed at similar ranges from the source. In fact, differences of 5 dB within small range intervals along the same bearing are not uncommon. This comparison typified the range-dependent characteristic of the bottom reverberation measured at the site and provided useful information into the nature of the scattering encountered during the experiment.

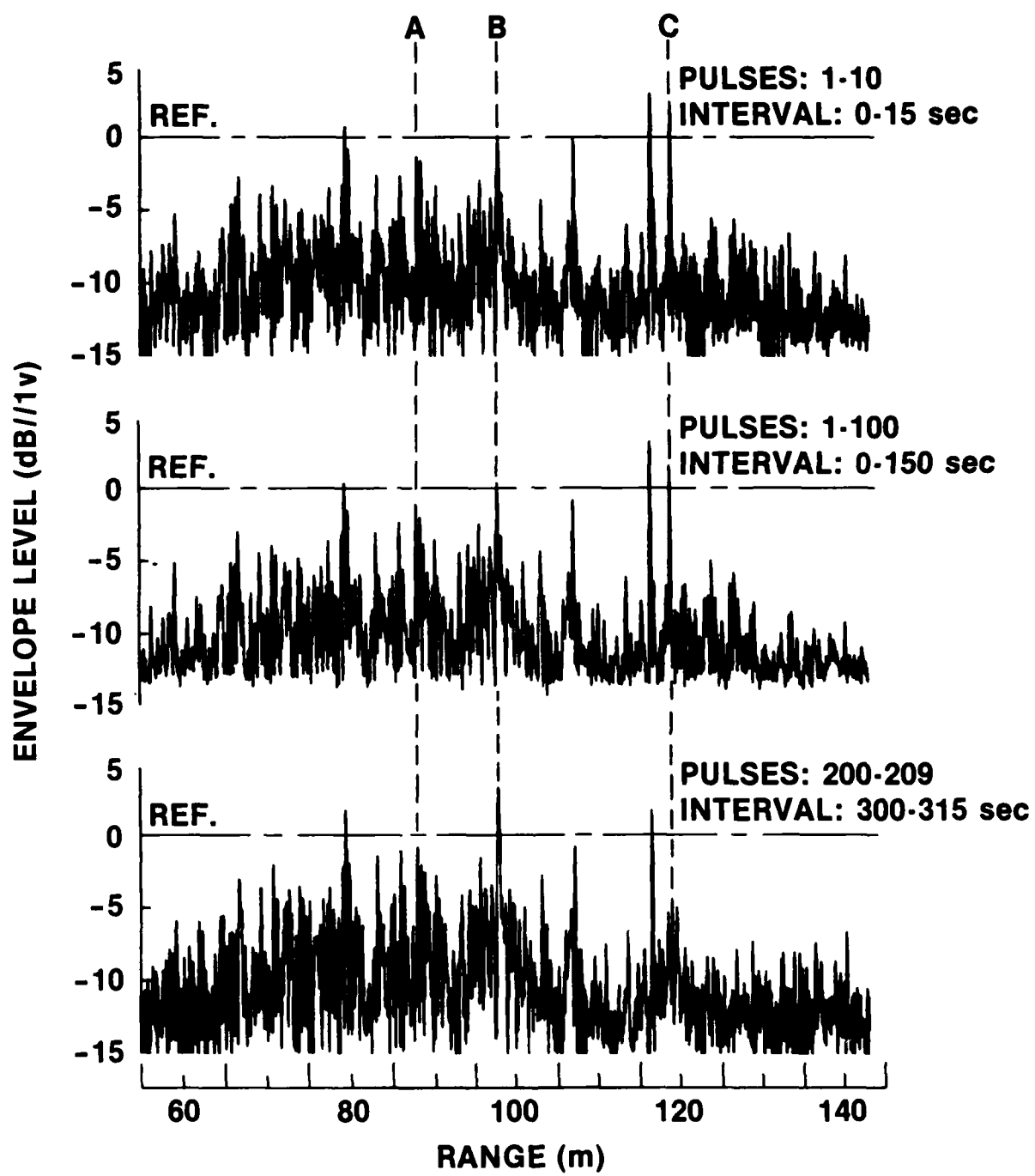


Figure 4. Bottom Reverberation vs. Range as a Function of Ensemble Interval  
(Frequency: 20 kHz, Pulse Width: 0.4 ms, Angle: 4°)

## TIME DEPENDENCE OF BOTTOM REVERBERATION

Additional insight into the bottom scattering mechanisms was provided by an aspect of the data analysis that was, at least initially, quite unexpected -- a time variability of the discrete scattering amplitudes (figure 4). The top figure in this comparison represents bottom reverberation obtained at 20 kHz from an ensemble average of the first 10 pulses of the measurement. This ensemble corresponded to an elapsed time interval of 15 seconds. In order to simplify the analysis, three individual scattering highlights (denoted A, B, and C) have been selected as a function of range. The middle figure represents a 100-pulse average corresponding to a 2.5 minute interval. The three scattering amplitudes are in excellent agreement with those of the top figure. The major difference between the top two figures is the expected decrease in the noise background as a result of the greater ensemble size. This observation contrasts sharply with the 10-pulse average presented in the bottom figure, which was obtained 5 minutes after the start of the measurements. Relative to the equivalent 0 dB reference lines, it is noted that, although scattering amplitude A remained constant for all three ensemble intervals, amplitude B increased 4 dB and amplitude C decreased 7 dB.

In general, the maximum duration of individual bottom-related measurements was 6 minutes. A detailed analysis of the various data sets as a function of the grazing angle, azimuth, and pulse width has revealed that many (if not most) of the predominant scattering highlights had significant time varying amplitudes as described here. Naturally, this effect immediately suggests a biological influence -- a topic which will be explored later in this paper.

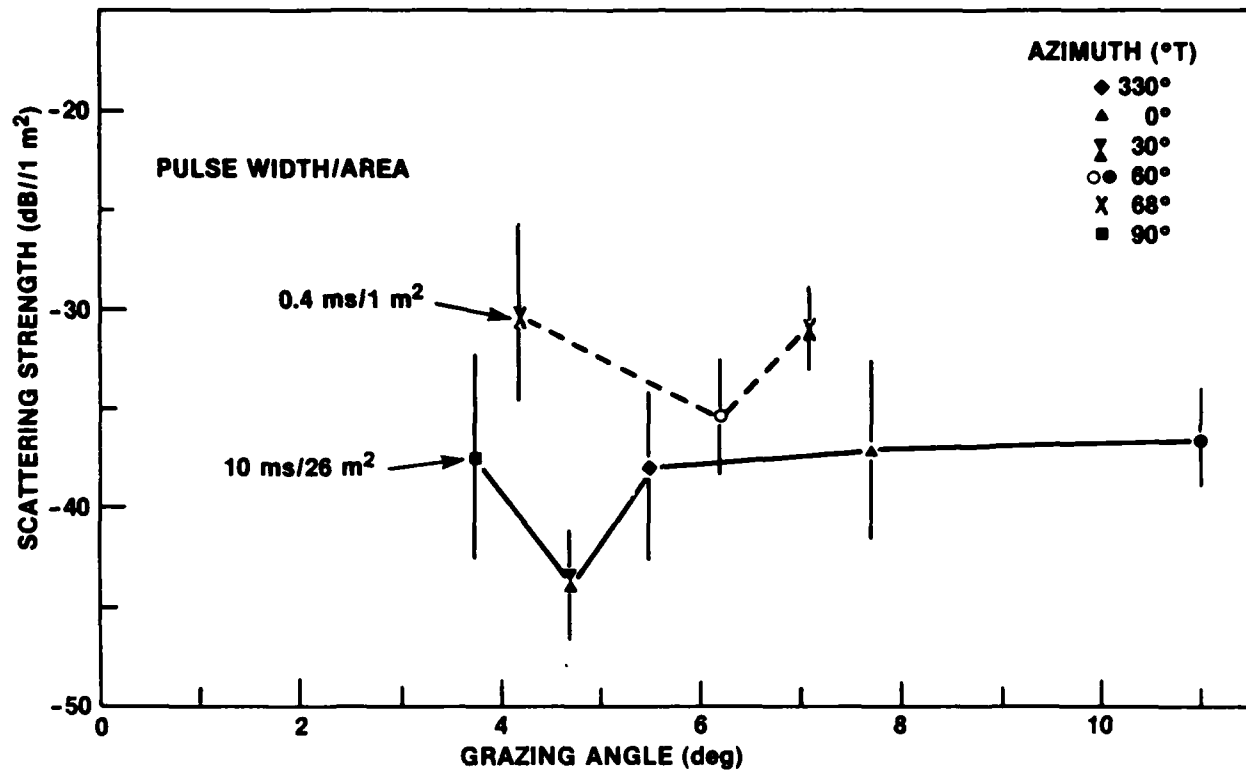


Figure 5. Bottom Scattering Strength (20 kHz) vs. Grazing Angle as a Function of Pulse Width and Azimuth

## BOTTOM SCATTERING STRENGTH VERSUS GRAZING ANGLE

In figure 5, bottom scattering strengths at 20 kHz, which were computed as a function of two pulse widths and various azimuth angles, are plotted versus bottom grazing angle. The vertical bars denote the range of maximum-to-minimum scattering strength values for scattering highlights located within  $\pm 0.5^\circ$  of the indicated grazing angle. In effect, these bars represent a measure of the range-dependent (or nonhomogeneous) bottom roughness conditions as shown in the previous two figures. Relative to the mid-range values denoted by the symbols, the scattering strength variations are the order of  $\pm 2$  to  $\pm 5$  dB.

Two important scattering strength characteristics may be inferred from the data: first, a pulse width dependence is apparent, and secondly, a lack of strong grazing angle dependence is indicated. This is not typical for reverberation from homogeneous boundaries as scattering strength relative to a unit area of insonification is generally independent of pulse width. However, the bottom encountered in this experiment was nonhomogeneous and patchy. Thus, increasing the pulse width caused the longer pulses to spatially average the discrete scatterers and perhaps encompass bottom areas larger than the patch size, thereby resulting in lower scattering strengths. A weak angular dependence is generally indicative of large (or comparable) roughness relative to the acoustic wavelength.

As noted earlier, direct measurements of bottom scattering strengths at low grazing angles are scarce. However, Wong and Chesterman [3] reported bottom scattering strengths that were inferred from an analysis of the time decay of bottom reverberation measurements at 48 kHz for pulse widths from 0.4 to 2.8 ms. For sandy sediments, they derived scattering strengths for grazing angles between  $2^\circ$  and  $4^\circ$  of approximately -30 dB with standard deviations varying from  $\pm 2$  to  $\pm 8$  dB. With respect to the limitations inherent in the analysis of reverberation decay rates, the general agreement with scattering strength values presented here is considered excellent.

TD 7181

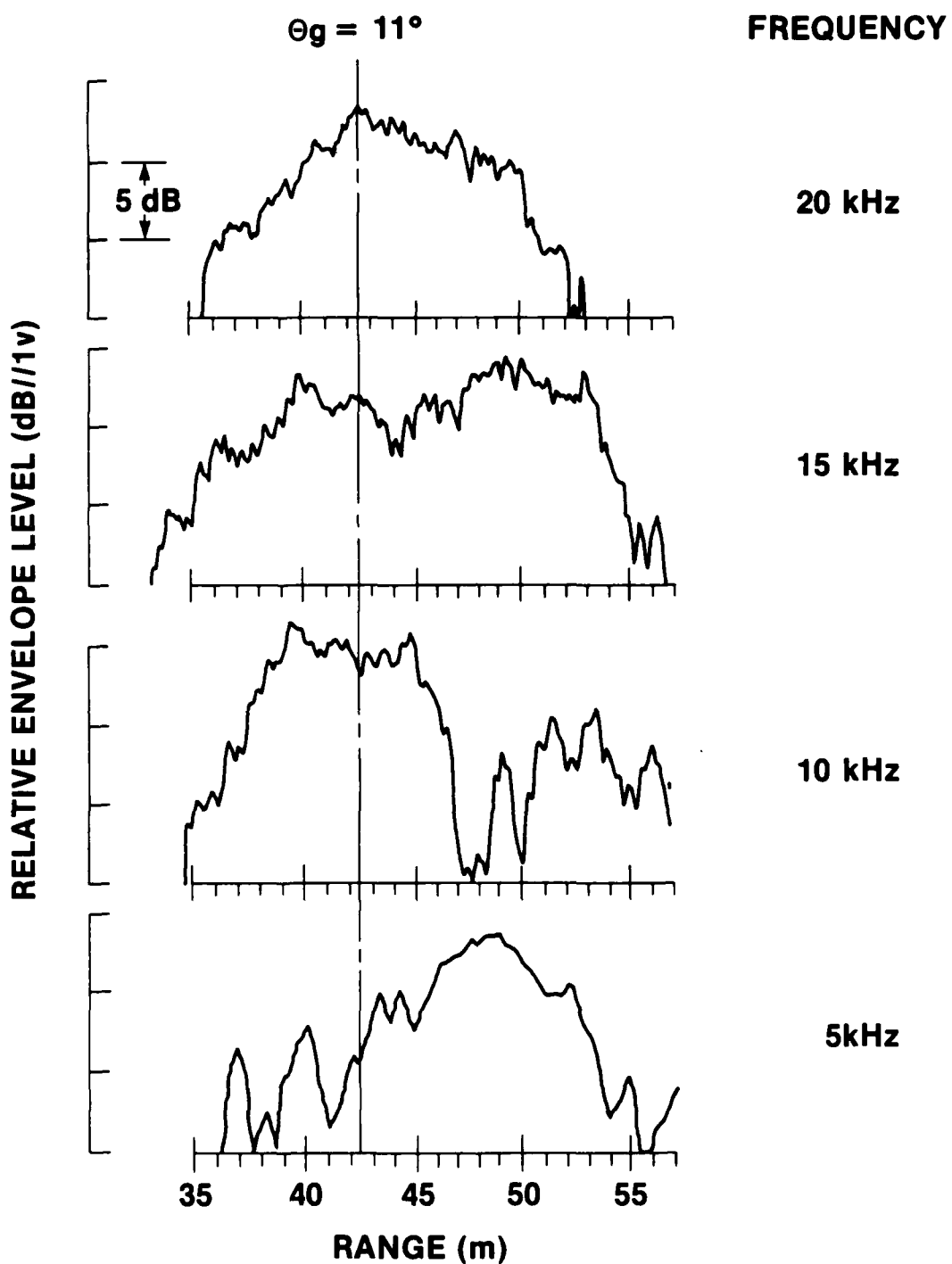


Figure 6. Bottom Reverberation vs. Range at Four Frequency  
(Pulse Width: 10 ms, Ensemble: 200 pulses)

## FREQUENCY VARIATIONS

A frequency comparison of reverberation levels versus range (figure 6) provides a qualitative appreciation of the complexities related to scattering effects from rough boundaries. These data are from narrow angular regions ( $\pm 3^\circ$ ) about the source's MRA at  $11^\circ$  grazing. At all frequencies, the noise levels are 10 to 15 dB below the reverberation levels shown here.

The levels for these 10 ms pulses contrast with the previous examples for 0.4 ms pulses. The increased spatial averaging results in a smoother representation of the discrete scattering highlights. With the exception of 5 kHz, a large scattering concentration occurs at a range of 42 m. The dominant scattering level for 5 kHz appears at 49 m, and it is suspected that this frequency may be influenced by sub-bottom scattering effects.

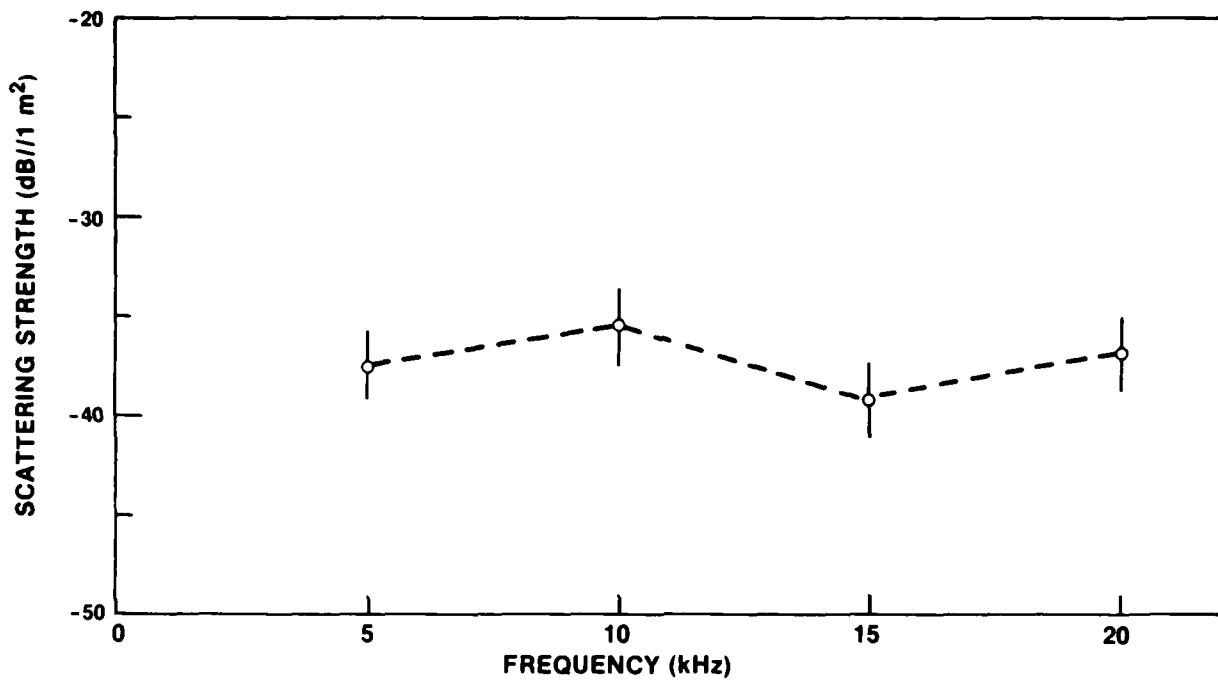


Figure 7. Bottom Scattering Strength vs. Frequency  
(Grazing Angle: 11°, Pulse Width: 10 ms, Ensemble: 200 Pulses)

Interestingly, the bottom scattering strengths at  $11^\circ$  grazing (figure 7), which correspond to the reverberation levels of the previous figure, exhibit a lack of frequency dependence. As before, the vertical bars represent the range in values within  $\pm 0.5^\circ$  of the grazing angle associated with the MRA of the parametric source. The relatively small variation of  $\pm 2$  dB is attributed to two factors. The spatial separation between the angular limits of  $10.5^\circ$  and  $11.5^\circ$  is minimal ( $\sim 4$  m). Also, the 10 ms pulse results in a 50% overlap of the insonified area for this separation. The combination of these two factors reduces the range dependent variability that is generally greater for lower grazing angles.

A weak frequency dependence is also an indication of large roughness conditions.

TD 7181

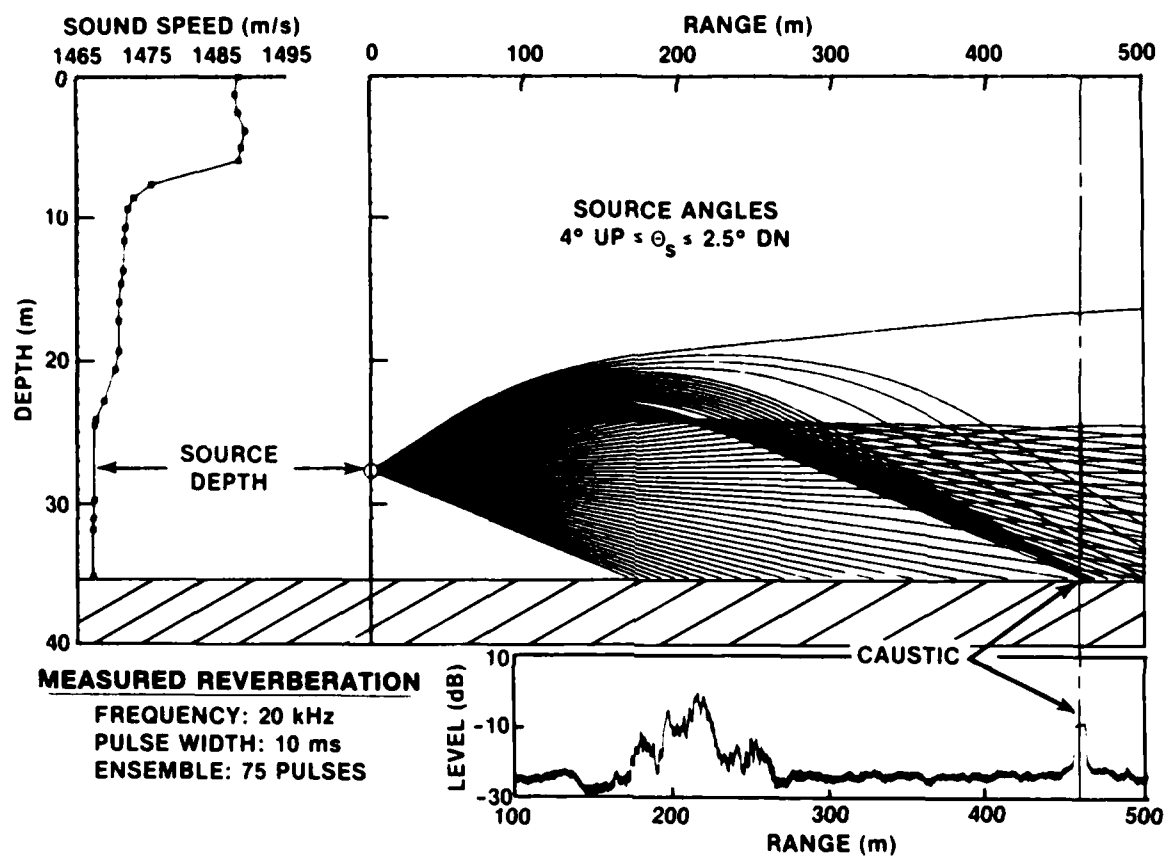


Figure 8. Coherent and Incoherent Bottom Reverberation

## COHERENT AND INCOHERENT BOTTOM REVERBERATION

The property of time dispersion in boundary reverberation following a particular law, such as decaying at a range of  $t^{-3}$ , will be affected not only by the vertical beam pattern of the transmitter/receiver combination, but also by the refractive conditions within the ocean medium. This can have important implications in determining the characteristics of the reverberated signal. For example, the ray plot shown in figure 8 was predicted from the measured sound velocity profile shown on the left side. The tracings were computed for rays leaving the projector between the angles of up  $4^\circ$  and down  $2.5^\circ$ . It can be seen that, under these downward refractive conditions, the rays that leave the source at a slight upward angle are focused and a caustic is formed on the bottom at a range of approximately 460 m. In the bottom portion of the figure, the measured reverberation is shown as a function of range. First, the bottom backscatter in the range interval 170 to 270 m is the energy received from the bottom along the maximum response axis of the source/receiver. However, the signal return at an approximate range of 460 m shows negligible time dispersion and has the characteristics of a coherent return from a point target. Thus, a highly refractive medium can focus the incident energy into a boundary with high intensity over a narrow range extent and produce a high level reverberation with small time dispersion. Similar results to those shown here were obtained at other azimuthal angles.

TD 7181

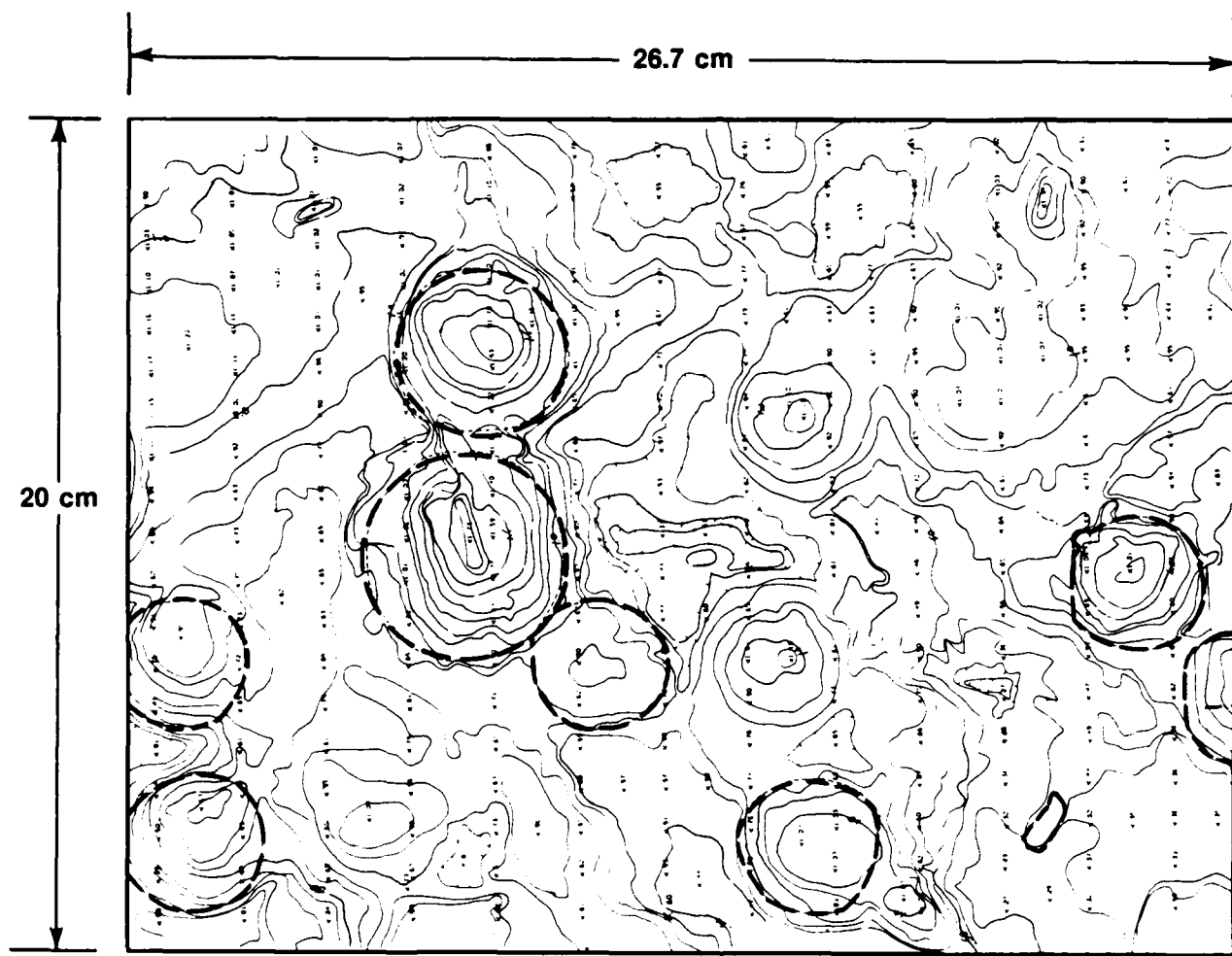


Figure 9. Example of Bottom Topography at the Experimental Site

## BOTTOM CONTOUR AND CORRESPONDING ROUGHNESS SPECTRUM

Scuba divers swam along a section of the ocean floor and took overlapping stereo photographs of the bottom topography. The stereo pairs were processed at an aerial cartographic laboratory to produce contours of the bottom roughness. A sample of the contour mapping is shown in figure 9. The standard deviation of the bottom roughness was computed along 1 m length parallel tracks and a typical value of 0.2 cm was obtained. This low value of bottom roughness may be explained by the presence of macrobenthic life forms that are known to smooth the ocean bottom.

The dominant life form collected during the experiment was a species of sand dollar known as Echinorachnius Parma [4]. Their presence, shown here by the dashed circular lines, was recorded at 75% of the sampled stations with estimated densities varying from 40 to 600 individuals per square meter. The average diameter of all species at the site was 4.5 cm. General scientific measurements suggest that sand dollar densities are inversely proportional to their size. The composition of E. Parma is 92% calcium carbonate [5], which has a specific density of 2.93 grams/cm<sup>3</sup>. This would make the sand dollar an excellent reflector of acoustic energy - relatively superior to the good reflective properties of the surrounding sandy sediments that had specific densities [4] from 2.05 to 2.37 grams/cm<sup>3</sup>. All of the evidence to date points to E. Parma as a prime candidate for describing the bottom scattering measurements of the experiment.

TD 7181

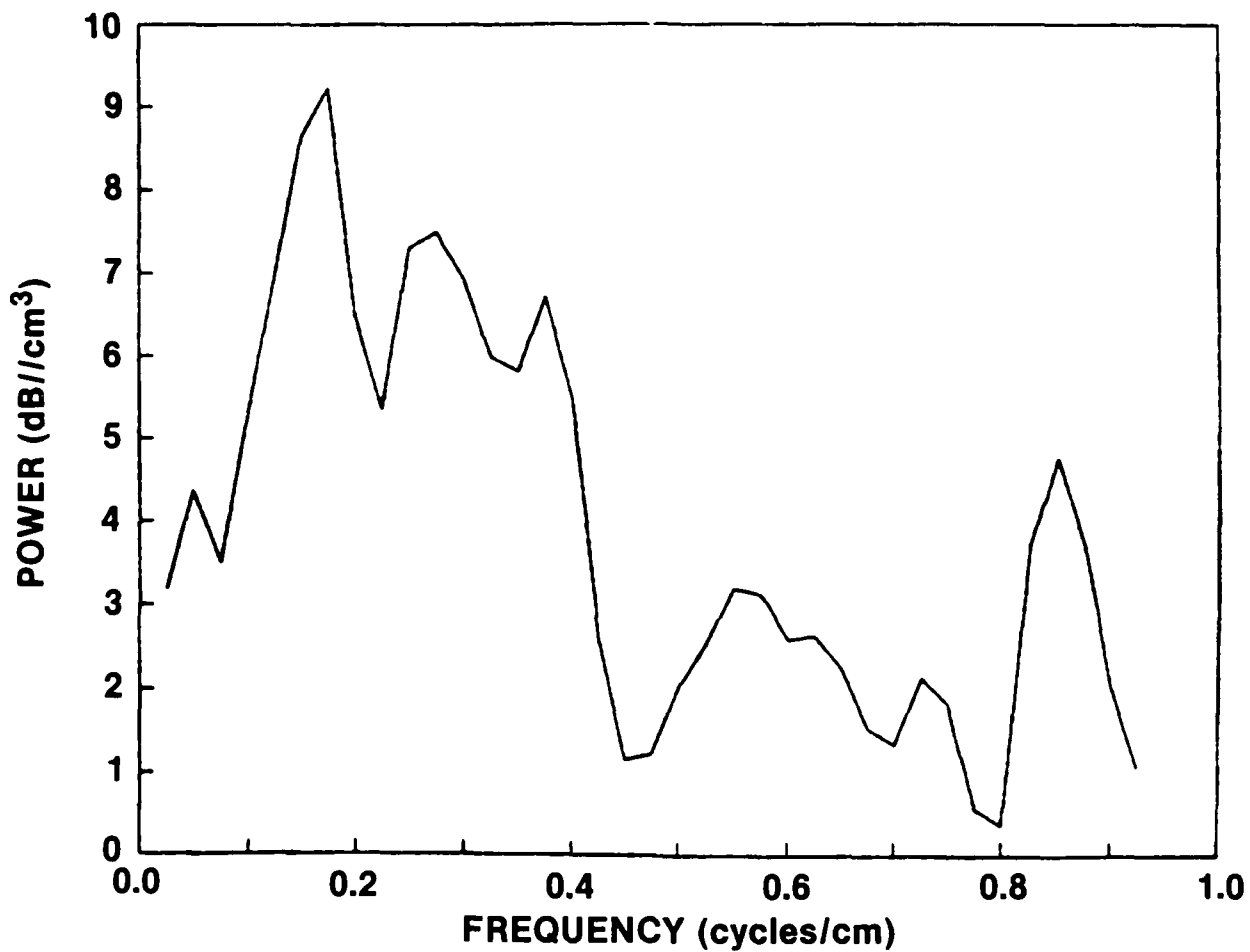


Figure 10. Bottom Roughness Spectrum

The bottom contour plots were digitized in 0.5 cm intervals and Fourier transformed to estimate the bottom micro-roughness spectra. Shown in figure 10 is an ensemble averaged roughness spectrum obtained from an average of 11 parallel tracks. The tracks were approximately 0.7 m in length. The peak spectral energy occurs at a spatial wavenumber of 0.175 cycles/cm, which corresponds to a period of 5.7 cm. This dimension is approximately the size of the sand dollars. The multipeaks in the spectrum are believed to be related to the percentage of sand dollars that do not have their diameters aligned along the tracks. The spectra are still undergoing analysis, where we are increasing the length of the tracks, computing multidimensional roughness spectra, and spatial correlation functions.

TO 7181

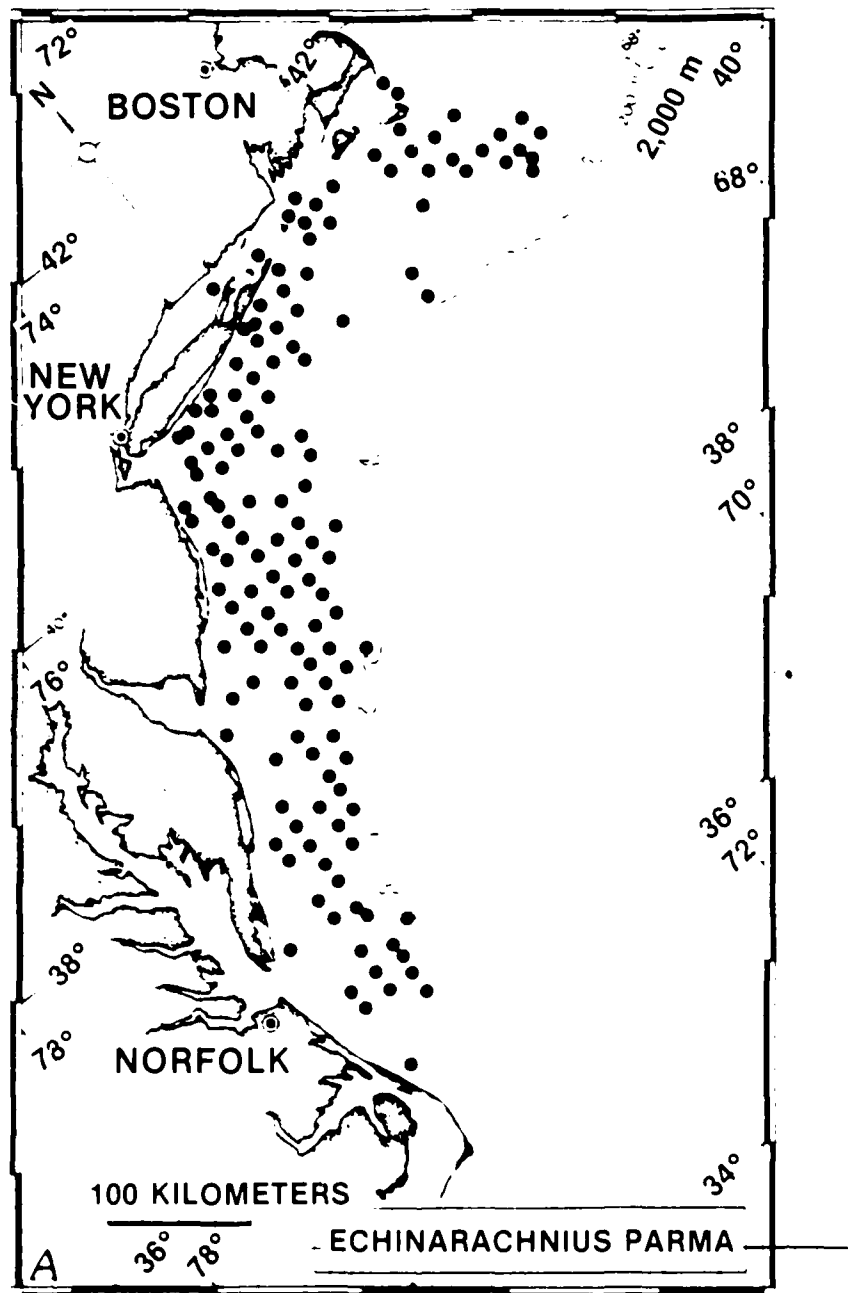


Figure 11. Sand Dollar Distribution  
(From Wigley and Theroux [6])

## SAND DOLLAR DISTRIBUTION

Geological surveys [6] conducted by the National Oceanic and Atmospheric Administration reveal that E. Parma is an amazingly prolific inhabitant of the continental shelf of the western North Atlantic (figure 11). Its known range extends from Cape Hatteras to Labrador and Greenland; and in some locations, it has been found in water depths of 2500 m. It is also found in the North Pacific. In the more extensive surveys [7], bottom contour intervals of sand dollar densities are measured in terms of hundreds of square miles. Other species of sand dollars inhabit the shelf areas of most of the world's ocean.

The maximum height of the sand dollar is approximately one-fourth of its diameter. However, it is a known practice of the sand dollar to bury the lower third of its body leaving the remainder of its shell protruding at sharp angles from the ocean bottom. This could be a contributing mechanism that accounts for relatively high scattering levels at low grazing angles.

## SUMMARY

- BOTTOM SCATTERING PROCESSES SIGNIFICANTLY INFLUENCED BY MACROBENTHOS OF SITE (CANDIDATE-SAND DOLLAR)
- REFRACTION IN THE MEDIUM CAN SIGNIFICANTLY ALTER THE REVERBERATION CHARACTERISTICS
- LACK OF STRONG FREQUENCY ( $5 \text{ kHz} \leq f \leq 20 \text{ kHz}$ ) OR GRAZING ANGLE ( $4^\circ \leq \Theta_g \leq 11^\circ$ ) DEPENDENCE
- RANGE AND PULSE WIDTH DEPENDENCE DUE TO NON-HOMOGENEOUS CONCENTRATION OF SCATTERERS
- EXPERIMENT CONFIRMS THE IMPORTANCE OF MULTIPLE ACOUSTIC MEASUREMENTS SUPPORTED BY EXTENSIVE ENVIRONMENTAL MEASUREMENTS

Figure 12. Bottom Reverberation Summary Highlights

## SUMMARY AND CONCLUSIONS

The acoustic, oceanographic, and geoacoustic data sets collected during this experiment are important to understanding the properties of acoustic bottom backscatter in a shallow water environment under either refractive or isovelocity conditions. The observations of weak dependence of scattering strength on acoustic frequency and grazing angle coupled with the low topographic bottom roughness but high concentration of sand dollars leads us to the following conclusion (see also figure 12):

The scattering is caused predominantly by a random distribution of highly reflective scatterers, biologic in origin and distributed on the surficial ocean bottom and into the sand sediment to a depth of several centimeters. The recent theoretical work of Victor Twersky [8], which treats the coherent and incoherent scatter from random distributions of protuberances, including hemi-ellipsoids with defined packing density, should be applicable to predicting the acoustic backscatter at these low grazing angles.

LIST OF REFERENCES

- [1] W. I. Roderick, J. B. Chester, and R. K. Dullea, High Frequency Backscatter from the Sea Surface, NUSC Technical Document 7183 (in preparation).
- [2] M. D. Richardson (NORDA), "Environmental Bottom Characterization Required for Modeling and Predictions of High-Frequency Acoustic Bottomscattering." Paper presented at the 107th meeting of the Acoustical Society of America, 9 May 1984.
- [3] H. K. Wong and W. D. Chesterman, "Bottom Backscattering Near Grazing Incidence in Shallow Water," Journal of the Acoustical Society of America, vol. 44, 1968, pp. 1713-1718.
- [4] M. D. Richardson, J. H. Tietjen (CCNY), and R. I. Ray, Environmental Support for Project WEAP East of Montauk Point, New York, 7-28 May 1982, NORDA Report 40, October 1983.
- [5] Personal correspondence from F. Steimle, NOAA Northeast Fisheries Center, Serial Letter F/NEC4:FS of 9 April 1984.
- [6] R. L. Wigley and R. B. Theroux, "Atlantic Continental Shelf and Slope of the United States -- Macrobenthic Invertebrate Fauna of the Middle Atlantic Bight Region -- Faunal Composition and Quantitative Distribution," Geological Survey Professional Paper 529-N, U.S. Government Printing Office, Washington, 1981.
- [7] J. V. Caracciolo and F. W. Steimle, Jr., An Atlas of the Distribution and Abundance of Dominant Benthic Invertebrates in the New York Bight Apex with Review of Their Life Histories, NOAA Technical Report NMFS SSRF-766, March 1983.
- [8] V. Twersky, "Reflection and Scattering of Sound by Correlated Rough Surfaces," Journal of the Acoustical Society of America, vol. 73(1), January 1983.

INITIAL DISTRIBUTION LIST

Addressee	No. of Copies
NAVSEASYS.COM (SEA-63R, D. Porter, C. Smith)	2
NORDA (Code 530, E. Chaika, B. Blumenthal; 113, R. Martin, W. Carey; 115, R. Farwell)	5
SACLANTCTR (Tech. Director, R. Goodman; T. Goldsberry)	2
ONR (CAPT E. Young; Code 4250A, M. McKisic; 425UA, T. Fitzgerald; 425, D. Bradley; 422CB, E. Hartwig)	5
ARL/PSU (S. McDaniel, D. McCammon)	2
APL/UW (C. Sienkiewicz)	1
ARL/UT (H. Bocheme)	1
NOAA/NFC (F. Steimle)	1
NOSC (B. Smith)	1
NRL (E. Franchi, B. Adams)	2
ONT (CAPT J. Harlett)	1
University of Illinois (V. Twersky)	1
FWG/Kiel, Germany (G. Ziehm, H. Herwig, B. Nuetzel)	3